Regioselective Synthesis of η^4-Dienylphosphane Ruthenium Complexes by Oxidative Coupling Reactions

J. Díez,[†] M. P. Gamasa,*[,†] E. Lastra,*[,†] A. Villar,[†] and E. Pérez-Carreño[‡]

Departamento de Química Orgánica e Inorgánica, Instituto de Química Organometálica "Enrique Moles" (Unidad Asociada al CSIC), Universidad de Oviedo, Oviedo, Principado de Asturias, Spain, and Departamento de Química Física y Analítica, Universidad de Oviedo, Oviedo, Principado de Asturias, Spain

Received May 14, 2007

Complexes [Ru(η^5-C_5H_5){κ^3(*P*,*C*,*C*)-$Ph_2P(CH_2)_nCH{=}CH_2$}(MeCN)][PF_6] (n = 1 (**1**), 2 (**2**)) react with C≡C bonds of propargylic alcohols to yield regioselectively the complexes [Ru(η^5-C_5H_5){κ(*P*),η^4-$Ph_2P(CH_2)_nCH{=}CHC(R){=}CH_2$}][$PF_6$] ($n$ = 1, R = CPh_2OH (**3**), $C(C_{12}H_8)OH$ (**4**), $C(C_4H_8)OH$ (**5**), CMePhOH (**6a**, **6b**); n = 2, R = CPh_2OH (**7**), $C(C_4H_8)OH$ (**8**), CMePhOH (**9a**, **9b**), CHPhOH (**10a**, **10b**)). The reaction of complex **1** with terminal alkynes also leads regioselectively to the complexes [Ru(η^5-C_5H_5)-{κ(*P*),η^4-(2*Z*,4*E*)-$Ph_2PCH_2CH{=}CHCH{=}CH(R)$}][$PF_6$] (R = Ph (**11**), *p*-$MeC_6H_4$ (**12**)). Single-crystal X-ray diffraction analyses for complexes **9a**, **9b**, **10b**, and **12** have been carried out and allow the unambiguous assignment of the stereochemistry of the complexes. DFT calculations regarding the thermodynamic stability of the obtained products have also been performed.

Introduction

We have previously reported that ruthenium(II) complexes [Ru(η^5-C_nH_m)(PPh_3){κ^3(*P*,*C*,*C*)-$Ph_2PCH_2CH{=}CH_2$}][PF_6] (C_nH_m = C_9H_7, C_5H_5)[1] react with alkynes and propargylic alcohols to give ruthenaphosphabicycloheptene complexes under mild thermal conditions (Chart 1). These reactions take place through the formation of vinylidene or allenylidene derivatives, which undergo an unusual diastereoselective [2+2] intramolecular cycloaddition with allyl C=C double bonds to generate the cyclobutylidene ring.[2] The progress of the reaction reflects the hemilabile character of the allyldiphenylphosphane ligand, a fact that has been corroborated by kinetic studies.[3]

On the other hand, intermolecular reactions between alkenes and alkynes (ene-type reactions or [2+2] coupling reactions) promoted by transition metal complexes are among the most efficient and selective methods for C−C bond formation.[4] In spite of the great development in this area, few examples of the reaction between alkynes and double bonds linked to the metal atom have been reported. Thus, the reactions between alkenylphosphane complexes of group 8 metals and terminal alkynes have been described in recent papers. Cyclopentadienylosmium(II) complexes promote the transformation of vinyl phosphane in dienylphosphaneosmium(II) derivatives [Os(η^5-C_5H_5)Cl{κ^3(*P*,*C*,*C*)-^{i}$Pr_2PC(=CH_2)CH_2CH{=}CH(Ph)$}] through an ene-type reaction.[5] An intramolecular version of this reaction has also been described.[6] Kirchner et al. have reported the coupling of alkynes with coordinated alkenyl phosphanes in the complex [Ru(η^5-C_5H_5){κ^3(*P*,*C*,*C*)-$Ph_2PCH_2CH_2CH{=}CH_2$}-(MeCN)][PF_6], leading to a mixture of dienylphosphane complexes.[7] Also, an alkyne−alkene coupling involving the complex [Ru(Tp){κ^3(*P*,*C*,*C*)-$Ph_2PCH{=}CHC(Ph){=}CH_2$}Cl] has also been reported.[8]

Chart 1

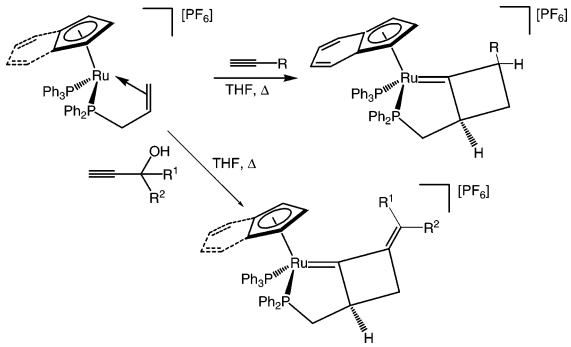

In this context, we report here the synthesis of novel cyclopentadienyl ruthenium(II) complexes containing the allyldiphenylphosphane ligand $Ph_2PCH_2CH{=}CH_2$ as well as their coupling reaction with the C≡C bonds of terminal alkynes and propargylic alcohols. The coupling reaction of the analogous complex containing the homoallyldiphenylphosphane ligand[7] [Ru(η^5-C_5H_5){κ^3(*P*,*C*,*C*)-$Ph_2PCH_2CH_2CH{=}CH_2$}(MeCN)]-[PF_6] and propargylic alcohols is also reported.

* Corresponding author. E-mail: pgb@uniovi.es (M.P.G.) and elb@uniovi.es (E.L.).

[†] Departamento de Química Orgánica e Inorgánica, Instituto de Química Organometálica "Enrique Moles".

[‡] Departamento de Química Física y Analítica.

(1) (a) Alvarez, P.; Lastra, E.; Gimeno, J.; Braña, P.; Sordo, J. A.; Gómez, J.; Falvello, L. R.; Bassetti, M. *Organometallics* **2004**, *23*, 2956−2966. (b) Díez, J.; Gamasa M. P.; Gimeno, J.; Lastra, E.; Villar, A. *Eur. J. Inorg. Chem.* **2006**, 78−87.

(2) (a) Álvarez, P.; Lastra, E.; Gimeno, J.; Bassetti, M.; Falvello, L. R. *J. Am. Chem. Soc*. **2003**, *125*, 2386. (b) Díez, J.; Gamasa, M. P.; Gimeno, J.; Lastra, E.; Villar, A. *Organometallics* **2005**, *24*, 1410−1418.

(3) Bassetti, M.; Álvarez, P.; Gimeno, J.; Lastra, E. *Organometallics* **2004**, *23*, 5127−5134.

(4) (a) Trost, B. M.; Toste, F. D.; Pinkerton, A. B. *Chem. Rev*. **2001**, *101*, 2067−2096. (b) Naota, T.; Takaya, H.; Murahashi, S.-I. *Chem. Rev.* **1998**, *98*, 2599−2660.

(5) Baya, M.; Buil, M. L.; Esteruelas, M. A.; Oñate, E. *Organometallics* **2005**, *24*, 2030−2038.

(6) Baya, M.; Buil, M. L.; Esteruelas, M. A.; Oñate, E. *Organometallics* **2005**, *24*, 5180−5183.

(7) Slugovc, C.; Mereiter, K.; Schmid, R.; Kirchner, K. *Organometallics* **1999**, *18*, 1011−1017.

(8) Slugovc, C.; Mereiter, K.; Schmid, R.; Kirchner, K. *Eur. J. Inorg. Chem.* **1999**, 1141−1149.

10.1021/om700476f CCC: $37.00
Publication on Web 09/19/2007

Scheme 1

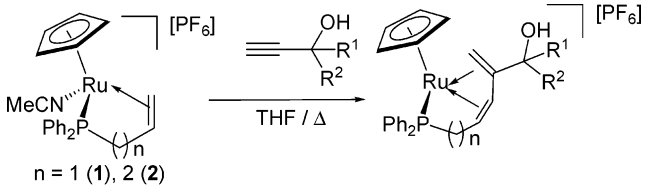

R^1, R^2 / n	Ph, Ph	$C_{12}H_8$	C_4H_8	Ph, Me	Ph, H
1	**3**	**4**	**5**	**6a,b**	-
2	**7**	-	**8**	**9a,b**	**10a,b**

Results and Discussion

Synthesis of [Ru(η^5-C_5H_5){κ^3(*P,C,C*)-$Ph_2PCH_2CH{=}CH_2$}(MeCN)][PF_6] (1). The air-stable cationic complex [Ru(η^5-C_5H_5){κ^3(*P,C,C*)-$Ph_2PCH_2CH{=}CH_2$}(MeCN)][PF_6] (**1**) has been prepared in 77% yield by the reaction of [Ru(η^5-C_5H_5)(MeCN)$_3$][PF_6] with allylphosphane in CH_2Cl_2 at 0 °C.

Complex **1** is soluble in CH_2Cl_2 and THF and insoluble in diethyl ether and *n*-hexane. Analytical and spectroscopic data (IR and ^{1}H, ^{13}C{^{1}H}, and ^{31}P{^{1}H} NMR) support the proposed formulation (see Experimental Section for details). The ^{31}P{^{1}H} NMR spectrum shows a singlet resonance at $\delta = -53.3$ ppm, in accordance with the values obtained for analogous κ^3-(*P,C,C*)-allylphosphane complexes [Ru(η^5-C_5H_5){κ^3(*P,C,C*)-Ph_2-$PCH_2CH{=}CH_2$}(PPh_3)][PF_6] ($\delta = -69.8$ ppm).[1b] Although the two olefin faces are diastereotopic, the coordination to the metal center is completely selective since the ^{31}P{^{1}H} and ^{1}H NMR spectra of complex **1** indicate the presence of a sole stereoisomer. This behavior has also been found for the complexes [Ru(η^5-C_9H_7){κ^3(*P,C,C*)-$Ph_2PCH_2CH{=}CH_2$}(PPh_3)][PF_6][1a] and [Ru(η^5-C_5H_5){κ^3(*P,C,C*)-$Ph_2PCH_2CH{=}CH_2$}(PPh_3)][PF_6].[1b]

Complexes [Ru(η^5-C_5H_5){κ^3(*P,C,C*)-$Ph_2PCH_2CH{=}CH_2$}-(MeCN)][PF_6] (**1**) and [Ru(η^5-C_5H_5){κ^3(*P,C,C*)-$Ph_2PCH_2CH_2$-$CH{=}CH_2$}(MeCN)][PF_6] (**2**) have been used as substrates in the reaction with propargylic alcohols. The synthesis of complex **2** has been previously reported.[7]

Regioselective Synthesis of [Ru(η^5-C_5H_5){κ(*P*),η^4-Ph_2P-$(CH_2)_n$$CH{=}CHC(R){=}CH_2$}][$PF_6$] (*n* = 1; R = CPh_2OH (3), $C(C_{12}H_8)OH$ (4), $C(C_4H_8)OH$ (5), CMePhOH (6); *n* = 2; R = CPh_2OH (7), $C(C_4H_8)OH$ (8), CMePhOH (9), CHPhOH (10)). The reaction of complexes [Ru(η^5-C_5H_5){κ^3(*P,C,C*)-Ph_2-$PCH_2CH{=}CH_2$}(MeCN)][PF_6] (**1**) and [Ru(η^5-C_5H_5){κ^3(*P,C,C*)-$Ph_2PCH_2CH_2CH{=}CH_2$}(MeCN)][PF_6] (**2**) with propargyl alcohols in refluxing THF leads to the formation of the complexes [Ru(η^5-C_5H_5){κ(*P*),η^4-(2*Z*)-$Ph_2PCH_2CH{=}CHC(R){=}CH_2$}]-[$PF_6$] (R = CPh_2OH (**3**), $C(C_{12}H_8)OH$ (**4**), $C(C_4H_8)OH$ (**5**), CMePhOH (**6**)) and [Ru(η^5-C_5H_5){κ(*P*),η^4-(3*Z*)-$Ph_2P(CH_2)_2$-$CH{=}CHC(R){=}CH_2$}][PF_6] (R = CPh_2OH (**7**), $C(C_4H_8)OH$ (**8**), CMePhOH (**9**), CHPhOH (**10**)), which are isolated as pink or white solids (Scheme 1). Complexes **6**, **9**, and **10** have been isolated as a mixture of two diastereoisomers as a consequence of the presence of a ruthenium and a carbon stereogenic center.

Complexes **3**−**10** are soluble in dichloromethane and insoluble in diethyl ether and *n*-hexane. All of them have been analytically and spectroscopically characterized (IR and ^{1}H, ^{31}P-{^{1}H}, and ^{13}C{^{1}H} NMR; see the Experimental Section for details). The most significant spectroscopic features are as follows: (i) The phosphorus signal for complexes **3**−**6** appears as a singlet between $\delta = -59.2$ and -61.9 ppm, while that of derivatives **7**−**10** is observed at $\delta = 95.1$ and 92.4 ppm. The formation of five- (**3**−**6**) and six-membered (**7**−**10**) ruthenaphosphacycles may account for the observed shift differences.[9] (ii) The ^{1}H NMR spectra show a doublet in the range 4.04−2.94 ppm ($J_{HH} = 5.2-3.5$ Hz) as well as a doublet of doublets in the range 1.42−0.70 ppm ($J_{HP} = 20.4-16.1$ and $J_{HH} = 5.2-3.5$ Hz), which are assigned to the geminal protons of the olefin group. (iii) The internal olefinic protons appear as multiplets at δ 6.49−4.72 ppm. The observed *J* values of ca. 8 Hz for complexes **7**−**10** are in agreement with the *Z* stereochemistry around the double bond. (iv) The signal for the terminal olefinic carbon in the ^{13}C{^{1}H} NMR spectra appears as a doublet at 44.4−38.9 ppm ($J_{CP} = 6.0-4.9$ Hz).

A plausible reaction mechanism that would rationalize the observed regio- and stereochemistry is shown in Scheme 2.

The generation of one coordination vacancy by MeCN dissociation followed by metal−alkyne π-coordination is assumed to be the first step. Once the alkyne is coordinated, an oxidative coupling with the double bond of the alkenyl ligand would lead to the ruthenacyclopentene intermediate (A), which gives the final complex via a β-elimination/reductive elimination sequence. Alternatively, the formation of the metal−alkyne complex might also occur by dissociation of the alkenylphosphane ligand. Thus, κ-P intermediates have been observed for the allylphosphane complexes **3**, **4**, **5**, and **6**, while no such species have been detected in the case of the complexes **7**, **8**, and **9** bearing the homoallylphosphane ligand. This fact is in agreement with the different hemilabile properties described for these ligands.[1−3]

X-ray Crystal Structure of the Complexes 9a·1/2OEt$_2$, 9b, and 10b·1/2OEt$_2$. Although complexes **6**, **9**, and **10** were obtained as a mixture of diastereoisomers, both diastereoisomers of complexes **9** and **10** were separated by recrystallization from dichloromethane/diethyl ether. In order to determine their stereochemistry, X-ray diffraction analyses of the diastereoisomers **9a**, **9b**, and **10b** have been carried out. Slow diffusion of diethyl ether into a solution of the complexes in dichloromethane

Scheme 2

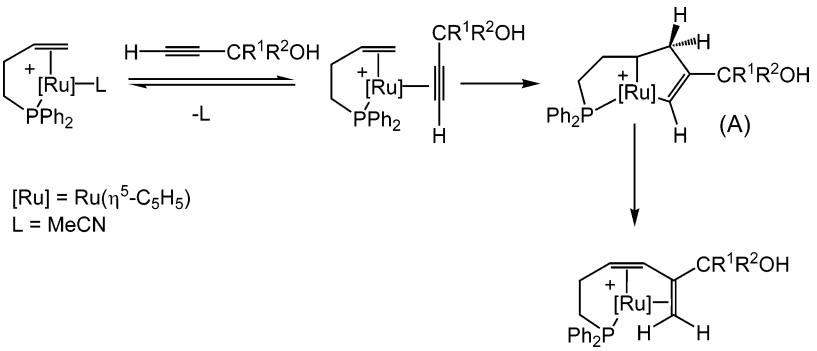

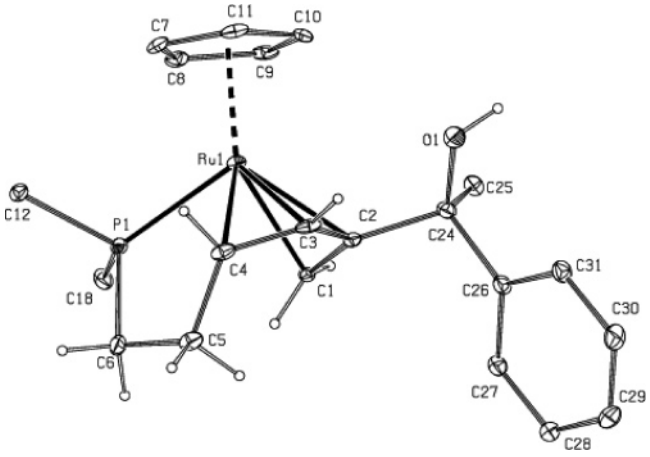

Figure 1. Molecular structure and atom-labeling scheme for complex **9a**·1/2OEt$_2$. Non hydrogen atoms are represented by their 20% probability ellipsoids. [PF_6] ion, most hydrogen atoms, phenyl rings, and solvent molecule have been omitted for clarity.

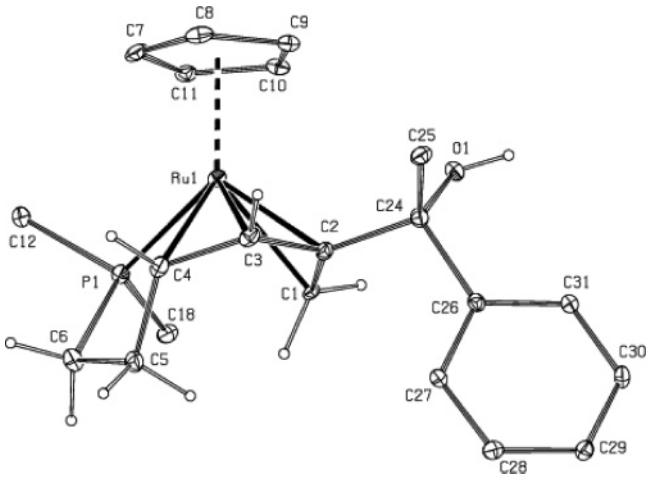

Figure 2. Molecular structure and atom-labeling scheme for complex **9b**. Non hydrogen atoms are represented by their 20% probability ellipsoids. [PF_6] ion, most hydrogen atoms, and phenyl rings have been omitted for clarity.

allowed us to collect suitable crystals for X-ray diffraction studies. An ORTEP-type representation of the cation of the complexes is shown in Figures 1−3. Selected bonding data are collected in Table 1.

The crystals belong to $P2_1/c$ (**9a**), *Cc* (**9b**), and $P2_1/n$ (**10b**) space groups, indicating the presence of the racemic mixture. For complex **9b** the asymmetric unit consists of two conformers that present identical stereochemistry with relative configuration $R_{Ru}R_C$. The relevant structural parameters are similar in both molecules, and the data corresponding to only one of them will be discussed.

All complexes exhibit a three-legged piano stool geometry, and the bond distances around the ruthenium atom are in accordance with previously reported structures (Å):[1b] Ru(1)−C* 1.8788(4) (**9a**), 1.881(16) (**9b**), 1.8635(3) (**10b**); Ru(1)−P(1) 2.304(1) (**9a**), 2.322(2) (**9b**), and 2.316(1) (**10b**). The C(3)−C(4) olefin atoms of the three structures adopt a *Z* configuration. The C(1)−C(2)−C(3)−C(4) atoms constitute a butadiene fragment in an *s-cis* conformation. The Ru−C(1), Ru−C(2), Ru−C(3), and Ru−C(4) bond distances reflect the coordination of the two olefins of this butadiene fragment to the metal center with distances in the range 2.253−2.150 Å.

(9) Garrou, P. *Chem. Rev.* **1981**, *81*, 229−266.

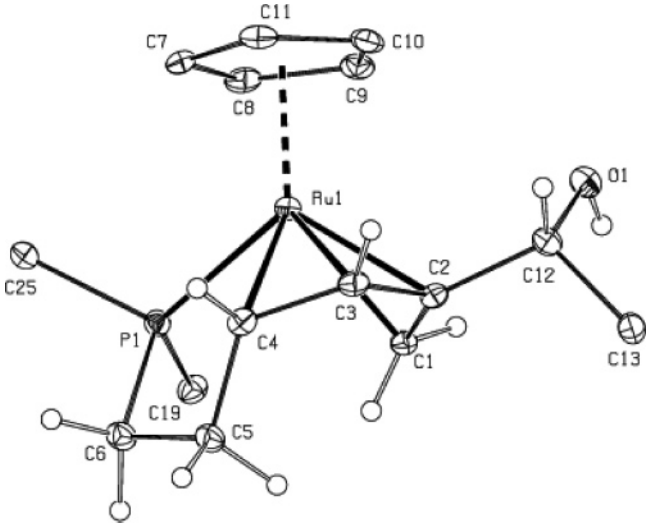

Figure 3. Molecular structure and atom-labeling scheme for complex **10b**·1/2OEt$_2$. Non hydrogen atoms are represented by their 20% probability ellipsoids. [PF_6] ion, most hydrogen atoms, phenyl rings, and solvent molecule have been omitted for clarity.

Table 1. Selected Bond Distances (Å) and Bond Angles (deg) for 9a·1/2OEt$_2$, 9b, and 10b·1/2OEt$_2$[a]

	9a·1/2OEt$_2$	**9b**	**10b**·1/2OEt$_2$
Bond Distances			
Ru(1)−C*	1.8788(4)	1.881(16)	1.8635(3)
Ru(1)−P(1)	2.3040(13)	2.3223(19)	2.3159(11)
Ru(1)−C(1)	2.208(5)	2.185(6)	2.197(4)
Ru(1)−C(2)	2.190(5)	2.187(6)	2.181(4)
Ru(1)−C(3)	2.150(5)	2.164(7)	2.172(4)
Ru(1)−C(4)	2.253(5)	2.241(7)	2.234(4)
C(1)−C(2)	1.419(7)	1.408(10)	1.421(6)
C(2)−C(3)	1.429(8)	1.418(10)	1.443(6)
C(3)−C(4)	1.395(8)	1.427(11)	1.415(5)
Bond Angles			
C*−Ru(1)−C(1)	138.54(14)	136.1(4)	134.81(12)
C*−Ru(1)−C(2)	128.65(13)	125.9(4)	125.36(12)
C*−Ru(1)−C(3)	128.08(14)	126.7(6)	126.50(12)
C*−Ru(1)−C(4)	137.32(11)	137.5(5)	138.03(12)
C*−Ru(1)−P(1)	117.14(4)	118.2(4)	117.90(3)
C(1)−C(2)−C(3)	119.3(5)	119.8(7)	121.0(4)
C(2)−C(3)−C(4)	123.1(5)	123.1(7)	121.9(4)

[a] C* = centroid of C(7), C(8), C(9), C(10), C(11).

The olefinic bond distances C(1)−C(2) and C(3)−C(4) are longer than that expected for a C=C, and the single C(sp^2)−C(sp^2) bond distance C(2)−C(3) is shorter than that of a single C−C bond, indicating some delocalization along the chain.

X-ray studies allow the unambiguous assignment of **9a** as the $R_{Ru}S_C$ diastereoisomer and of **9b** and **10b** as the $R_{Ru}R_C$ diastereoisomer. It is worth noting that a different diasteroisomer [**9b** ($R_{Ru}R_C$) and **10a** ($R_{Ru}S_C$)] crystallizes from the solutions of complexes **9** and **10**. Therefore, the X-ray diffraction studies were crucial to elucidate the structures of all of the resulting complexes.

Regioselective Synthesis of [Ru(η^5-C$_5$H$_5$){κ(*P*),η^4-(2*Z*,4*E*)-Ph$_2$PCH$_2$CH=CHCH=CH(R)}][PF$_6$] (R = Ph (11), *p*-MeC$_6$H$_4$ (12)). The reaction of complex [Ru(η^5-C$_5$H$_5$){κ^3(*P*,*C*,*C*)-Ph$_2$PCH$_2$CH=CH$_2$}(MeCN)][PF$_6$] (**1**) with RC≡CH (R = Ph, *p*-MeC$_6$H$_4$) in refluxing THF for 50 min yields regioselectively the complexes [Ru(η^5-C$_5$H$_5$){κ(*P*),η^4-(2*Z*,4*E*)-Ph$_2$PCH$_2$CH=CHCH=CH(R)}][PF$_6$] (R = Ph (**11**), *p*-MeC$_6$H$_4$ (**12**)) (Scheme 3).

Complexes **11** and **12** are obtained as pale yellow solids in 77% and 69% yield, respectively. Both complexes have been

Scheme 3

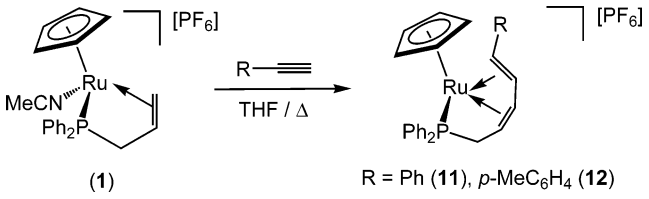

(**1**) R = Ph (**11**), *p*-MeC$_6$H$_4$ (**12**)

fully characterized by spectroscopic methods. Thus, the IR spectra show the characteristic $\nu(PF_6)$ band at 838 (**11**) and 839 cm^{-1} (**12**). The ^{1}H NMR spectra of both complexes show characteristic signals for the internal olefinic protons of the η^4-butadiene fragment in the range 6.97−4.95 ppm. The =CHR proton appears at lower fields (2.90 (**11**) and 2.91 (**12**) ppm) as a doublet of doublets (J_{HP} 15.5−15.4, J_{HH} 9.7−9.5 Hz). The ^{31}P{^{1}H} NMR spectra show the characteristic high-field signals for the ligand at −64.60 and −64.26 ppm for **11** and **12**, respectively. Other analytical and spectroscopic data are in agreement with the proposed formulations.

The most interesting feature in the reactions of complex **1** with terminal alkynes RC≡CH (R = Ph, *p*-MeC$_6$H$_4$) is the high regioselectivity observed, unlike the reaction between **2** and alkynes reported by Kichner, where the linear dienyl regioisomer is formed along with the branched dienyl regioisomer.[7]

On the other hand, it is interesting to note that a reversed regioselectivity is observed in the reaction of complex **1** with alkynes and propargylic alcohols. Thus, complexes **11** and **12** result from alkynes (see Scheme 3), while complexes **3**−**6**, having a branched butadiene unit, are formed from propargylic alcohols (see Scheme 1).

X-ray Crystal Structure of the Complex [Ru(η^5-C$_5$H$_5$)-{κ(*P*),η^4-(2*Z*,4*E*)-Ph$_2$PCH$_2$CH=CHCH=CH(*p*-MeC$_6$H$_4$)}][PF$_6$] (12). Slow diffusion of *n*-hexane into a solution of the complex **12** in dichloromethane allowed us to collect suitable crystals for X-ray diffraction studies. An ORTEP-type representation of the cation is shown in Figure 4, and selected bonding data are collected in the caption.

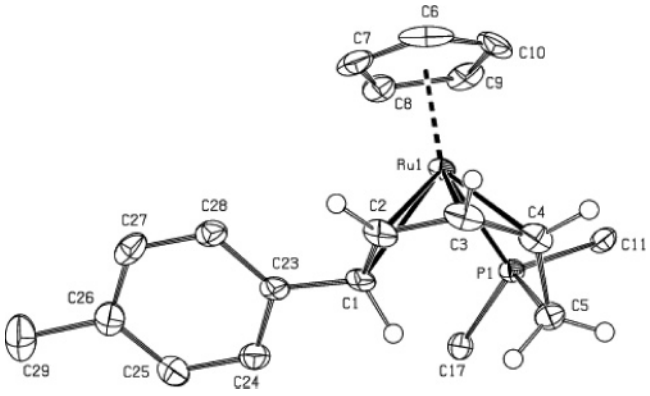

Figure 4. Molecular structure and atom-labeling scheme for complex **12**. Non hydrogen atoms are represented by their 20% probability ellipsoids. [PF$_6$] ion, most hydrogen atoms, and phenyl rings have been omitted for clarity. Selected bond lengths (Å): Ru(1)−C* = 1.86226(19), Ru(1)−P(1) = 2.2938(7), Ru(1)−C(1) = 2.279(3), Ru(1)−C(2) = 2.165(3), Ru(1)−C(3) = 2.181(3), Ru(1)−C(4) = 2.277(3), C(1)−C(2) = 1.410(4), C(2)−C(3)= 1.437(4), C(3)−C(4) = 1.415(5). Selected bond angles (deg): C*−Ru(1)−C(1) = 135.71(7), C*−Ru(1)−C(2) = 128.62(8), C*−Ru(1)−C(3) = 131.14(8), C*−Ru(1)−C(4) = 138.33(8), C*−Ru(1)−P(1) = 125.827(19), C(1)−C(2)−C(3) = 122.6(3), C(2)−C(3)−C(4) = 125.5(3), C(3)−C(4)−C(5) = 127.8(3), C* = centroid of C(6), C(7), C(8), C(9), C(10).

Chart 2

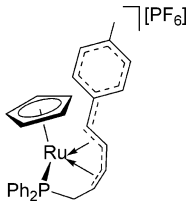

The crystals belong to a centrosymmetric space group, $P2_1/c$. Complex **12** exhibits a three-legged piano stool geometry with the ruthenium atom bonded η^5 to the cyclopentadienyl ring and to the phosphorus atom and η^2 to the two olefin groups of the dienylphosphane ligand. The bond distances around the ruthenium atom are in accord with previous structures.[1b] Like in complexes **9a**, **9b**, and **10b**, the butadiene fragment C(1)−C(2)−C(3)−C(4) of **12** presents an *s-cis* conformation and the Ru−C(1), Ru−C(2), Ru−C(3), and Ru−C(4) bond distances (2.279−2.165 Å) reflect the coordination of the two olefins to the metal center and are longer than those found for complexes **9a**, **9b**, and **10b**. The bond distances C(1)−C(2) (1.410(4) Å), C(2)−C(3) (1.437(4) Å), and C(3)−C(4) (1.415(5) Å) are relatively uniform, in accordance with electronic delocalization along the chain. For this complex, the C(1)−C(23) bond distance (1.486(4) Å) indicates that delocalization can also occur through the aromatic ring (see Chart 2). The torsion angles C(3)−C(2)−C(1)−C(23) and C(4)−C(3)−C(2)−C(1) (8.1(2)° and 4.9(4)°) agree with the planarity of the chain. The stereochemistry around the C(1)−C(2) and C(3)−C(4) double bonds are *E* and *Z*, respectively.

Theoretical Calculations. As shown before, the reaction of complexes **1** and **2** with propargylic alcohols leads to complexes that contain a branched butadiene fragment, while the reaction of **1** with RC≡CH (R = Ph, *p*-MeC$_6$H$_4$) yields complexes **11** and **12**, containing a linear butadiene fragment.

In order to understand the regiochemistry of these reactions, minimum-energy structure calculations were carried out by DFT methods. Calculations were performed on selected molecules isolated in the present work and on hypothetical ones.

No simplified model compounds were used for the calculations. Calculated structures are assigned Roman numbers. The isomers that present a branched dienylphosphane ligand are named as "a", and the complexes with a linear one are named as "b". Computer-generated images of all these structures are given as Supporting Information.

Table 2 shows the relative energies of optimized structures. The calculated more stable isomers are in accord with the experimental results, even when the energy differences are only 0.3 to 2.7 kcal mol^{-1}. Thus, complexes **6** (IIa), **9** (VIa), and **10** (VIIa), containing a branched dienylphosphane ligand, are more stable than the corresponding "b" isomers (IIb, VIb, and VIIb), having a linear dienylphosphane ligand. In order to know the influence of the OH group in the regiochemistry of the reaction, calculations for a hypothetical complex where the OH group is replaced by an H atom (V and X) were carried out. For both complexes the type "a" isomer with the linear dienylphosphane ligand is still the thermodynamically more stable isomer, pointing out that the OH group is not responsible for the observed regiochemistry. The same results were found for R = Me (complexes IV and IX). On the other hand, for complex **12** the regioisomer displaying the linear dienylphosphane ligand (IIIb) is 2.1 kcal mol^{-1} more stable than the IIIa isomer. The formation of complexes IIIb and VIIIb as the more stable isomers agrees with the stabilization due to the linear conjugation with the aromatic ring, which cannot occur with any other substituent.

Table 2. Relative Energies (kcal mol^{-1}) of DFT-Optimized Structures (0.0 kcal mol^{-1} is the energy assigned to the most stable isomer)

	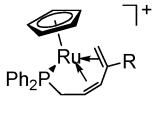	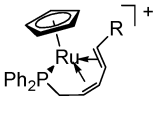	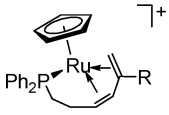	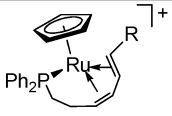
R	a	b	a	b
CH(Ph)OH	(Ia) 0.0	(Ib) 0.4	(VIa) 0.0 (**9**)	(VIb) 2.7
CMe(Ph)OH	(IIa) 0.0 (**6**)	(IIb) 0.3	(VIIa) 0.0 (**10**)	(VIIb) 2.2
p-MeC$_6$H$_4$	(IIIa) 2.1	(IIIb) 0.0 (**12**)	(VIIIa) 0.9	(VIIIb) 0.0
Me	(IVa) 0.0	(IVb) 0.7	(IXa) 0.0	(IXb) 1.3
CH$_2$Ph	(Va) 0.0	(Vb) 0.3	(Xa) 0.0	(Xb) 1.1

For complexes **9a**, **10a**, and **12**, the distances found for DFT-optimized structures are in agreement with the distances found by the X-ray analysis. So, DFT calculations can also be used to analyze structural aspects of the hypothetical complexes. Thus, according to the statement that the delocalization through the aromatic ring is an important factor for the higher stability of IIIb and VIIIb, the calculated distances C(2)−Cipso for the type "a" isomers (1.4915 Å for IIIa and 1.4905 Å for VIIIa) are longer than those calculated for the isomers of type "b" (1.4725 Å for IIIb and 1.4745 Å for VIIIb), in agreement with linear conjugation in type "b" isomers versus cross-conjugation in type "a" isomers.

Conclusions

In summarizing, the present work describes the synthesis of a series of complexes bearing η^4-dienylphosphane ligands via the C−C coupling of C≡C bonds with alkenylphosphanes. The X-ray structure of representative derivatives of these complexes allows the comparison between different alkenylphosphanes and alkynes showing different regioselectivity depending on the alkyne. Theoretical calculations have been carried out to explain the high regioselectivity of the process. Even when the differences in energy are low, it was found that regioselectivity agrees in all cases with the experimentally obtained complex.

Experimental Section

General Procedures. All manipulations were performed under an atmosphere of dry nitrogen using vacuum-line and standard Schlenk techniques. Solvents were dried by standard methods and distilled under nitrogen before use. The complexes [Ru(η^5-C$_5$H$_5$)(MeCN)$_3$][PF$_6$][10] and [Ru(η^5-C$_5$H$_5$){κ^3(*P,C,C*)-Ph$_2$PCH$_2$CH$_2$CH=CH$_2$}(MeCN)][PF$_6$][7] were prepared by previously reported methods. Other reagents were obtained from commercial suppliers and used without further purification. Infrared spectra were recorded on a Perkin-Elmer 1720-XFT spectrometer. The C, H, and N analyses were carried out with a Perkin-Elmer 240-B microanalyzer. Mass spectra (FAB) were recorded using a VG-Autospec spectrometer, operating in the positive mode; 3-nitrobenzyl alcohol (NBA) was used as the matrix. Mass spectra (MALDI-TOF) were determined with a Microflex Bruker spectrometer, operating in the positive mode; dihydroxyanthranol was used as the matrix. NMR spectra were recorded on Bruker AC 300 and 300 DPX instruments at 300.1 MHz (^{1}H), 121.5 MHz (^{31}P), or 75.4 MHz (^{13}C) and a Bruker AC 400 instrument at 400.1 MHz (^{1}H), 162.0 MHz (^{31}P), or 100.6 MHz (^{13}C) using SiMe$_4$ or 85% H$_3$PO$_4$ as standard. DEPT experiments were carried out for all the compounds reported. 2D-NMR (HSQC, HMBC) were performed in selected complexes. Coupling constants *J* are given in hertz. Abbreviations used: Ar, aromatic; s, singlet; d, doublet; dd, doublet of doublets; t, triplet; m, multiplet; br, broad. The ^{31}P NMR spectra of the complexes show the corresponding PF$_6$ septuplet signal. The following atom labels have been use for the ^{1}H and ^{13}C{^{1}H} NMR spectroscopic data:

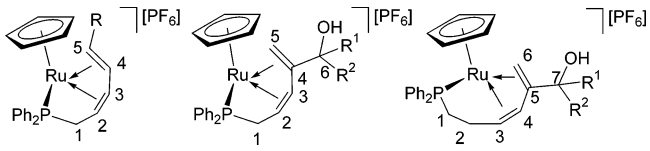

Synthesis of [Ru(η^5-C$_5$H$_5$){κ^3(*P,C,C*)-Ph$_2$PCH$_2$CH=CH$_2$}(MeCN)][PF$_6$] (1). A solution of [Ru(η^5-C$_5$H$_5$)(MeCN)$_3$][PF$_6$] (200 mg, 0.35 mmol) and allyldiphenylphosphane (82 μL, 0.38 mmol) in CH$_2$Cl$_2$ (35 mL) was stirred at 0 °C for 1.5 h. The solution was then evaporated to dryness, the crude product extracted with dichloromethane (2 × 10 mL), and the extract filtered. Concentration of the resulting solution to ca. 3 mL followed by the addition of 30 mL of diethyl ether precipitated a pale yellow solid, which was washed with diethyl ether (2 × 5 mL) and vacuum-dried. Yield: 156 mg, 77%. IR (Nujol, ν(PF$_6$), ν(CN), cm^{-1}): 839, 2968. Molar conductivity (acetone, Ω^{-1} cm^2 mol^{-1}): 106. ^{1}H NMR (300.1 MHz, CD$_2$Cl$_2$,18 °C): δ 2.01 (s, 3H, CH$_3$), 3.14 (m, 2H, P−CH$_2$, =CH$_2$), 3.95 (m, 1H, =CH$_2$), 4.43 (m, 2H, P−CH$_2$, =CH), 4.87 (s, 5H, C$_5$H$_5$), 7.40−7.65 (m, 10H, Ph). ^{13}C{^{1}H} NMR (100.6 MHz, acetone-*d*$_6$,18 °C): δ 2.9 (s, CH$_3$), 32.5 (d, J_{CP} = 34.2 Hz, P−CH$_2$), 45.9 (d, J_{CP} = 21.9 Hz, =CH), 52.8 (d, J_{CP} = 6.1 Hz, =CH$_2$), 82.8 (s, C$_5$H$_5$), 127.5−135.0 (CN, Ph). ^{31}P{^{1}H} NMR (121.5 MHz, CD$_2$Cl$_2$, 18 °C): δ −53.3 (s). C$_{22}$H$_{23}$F$_6$NP$_2$Ru (578.43 g/mol). MS (FAB+): *m*/*z* 393 [Ru(C$_5$H$_5$)(Ph$_2$PCH$_2$CH=CH$_2$)]$^+$.

Synthesis of [Ru(η^5-C$_5$H$_5$){κ(*P*),η^4-(2*Z*)-Ph$_2$PCH$_2$CH=CHC(R)=CH$_2$}][PF$_6$] (R = CPh$_2$OH (3), C(C$_{12}$H$_8$)OH (4), C(C$_4$H$_8$)OH (5), CMePhOH (6)). A solution of [Ru(η^5-C$_5$H$_5$){κ^3(*P,C,C*)-Ph$_2$PCH$_2$CH=CH$_2$}(MeCN)][PF$_6$] (58 mg, 0.1 mmol) and the corresponding propargyl alcohol (0.3 mmol) in THF (10 mL) was refluxed for 50 min. The solution was then evaporated to dryness, the crude product extracted with dichloromethane (2 × 10 mL), and the extract filtered. Concentration of the resulting solution to ca. 3 mL followed by the addition of 30 mL of diethyl ether afforded complexes **3**−**6** as pink solids, which were washed with diethyl ether (2 × 5 mL) and vacuum-dried. Yield of **3**: 59 mg, 79%. IR (KBr, ν(PF$_6$), cm^{-1}): 840. Molar conductivity (acetone, Ω^{-1} cm^2 mol^{-1}): 107. ^{1}H NMR (300.1 MHz, acetone-*d*$_6$, 18 °C): δ 1.42 (dd, J_{HP} = 20.4 Hz, J_{HH} = 5.2 Hz, 1H, H-5), 3.39 (m, 1H, H-1), 3.54 (d, J_{HH} = 5.2 Hz, 1H, H-5), 4.05 (m, 1H, H-1), 4.84 (m, 1H,

(10) Trost, B. M.; Older, C. M. *Organometallics* **2002**, *21*, 2544−2546.

H-2), 5.27 (s, 5H, C_5H_5), 5.62 (m, 1H, H-3), 6.00 (s, 1H, OH), 7.23−7.72 (m, 20H, Ph). $^{13}C\{^1H\}$ NMR (75.4 MHz, acetone-d_6, 18 °C): δ 28.8 (d, J_{CP} = 39.6 Hz, C-1), 43.7 (d, J_{CP} = 5.3 Hz, C-5), 44.9 (d, J_{CP} = 28.1 Hz, C-2), 82.7 (s, C-6), 87.9 (s, C_5H_5), 88.1 (d, J_{CP} = 4.7 Hz, C-3), 114.6 (s, C-4), 127.7−149.9 (Ph). $^{31}P\{^1H\}$ NMR (121.5 MHz, acetone-d_6, 18 °C): δ −61.9 (s). $C_{35}H_{32}F_6OP_2Ru$ (745.64 g/mol). MS (MALDI): *m*/*z* 601 [Ru(C_5H_5){Ph_2PCH_2CH═$CHC(CPh_2OH)$═CH_2}]$^+$. Yield of **4**: 54 mg, 73%. IR (KBr, $\nu(PF_6)$, cm^{-1}): 841. Molar conductivity (acetone, Ω^{-1} cm^2 mol^{-1}): 105. ^1H NMR (300.1 MHz, acetone-d_6, 18 °C): δ 0.70 (dd, J_{HP} = 19.8 Hz, J_{HH} = 4.7 Hz, 1H, H-5), 2.90 (m, 1H, H-1), 3.43 (d, J_{HH} = 4.7 Hz, 1H, H-5), 4.03 (m, 1H, H-1), 4.89 (m, 1H, H-2), 5.58 (s, 5H, C_5H_5), 5.74 (s, 1H, OH), 6.00 (m, 1H, H-3), 7.36−7.86 (m, 18H, Ph). $^{13}C\{^1H\}$ NMR (75.4 MHz, acetone-d_6, 18 °C): δ 28.5 (d, J_{CP} = 39.2 Hz, C-1), 40.0 (d, J_{CP} = 4.9 Hz, C-5), 45.4 (d, J_{CP} = 28.0 Hz, C-2), 84.8 (s, C-6), 85.1 (d, J_{CP} = 5.1 Hz, C-3), 87.9 (s, C_5H_5), 112.3 (s, C-4), 122.3−151.3 (Ph). $^{31}P\{^1H\}$ NMR (121.5 MHz, acetone-d_6, 18 °C): δ −61.6 (s). $C_{35}H_{30}F_6OP_2Ru$ (743.62 g/mol). MS (MALDI): *m*/*z* 599 ([Ru(C_5H_5){Ph_2PCH_2CH═$CHC(C(C_{12}H_8)OH)$═CH_2}]$^+$. Yield of **5**: 45 mg, 70%. IR (KBr, $\nu(PF_6)$, cm^{-1}): 841. Molar conductivity (acetone, Ω^{-1} cm^2 mol^{-1}): 109. ^1H NMR (300.1 MHz, acetone-d_6, 18 °C): δ 0.88 (dd, J_{HP} = 19.8 Hz, J_{HH} = 4.9 Hz, 1H, C-5), 1.85 (m, 6H, −$(CH_2)_4$−), 2.18 (m, 2H, −$(CH_2)_4$−), 3.02 (m, 1H, H-1), 3.66 (d, J_{HH} = 4.9 Hz, 1H, H-5), 4.01 (m, 1H, H-1), 4.75 (m, 1H, H-2), 5.09 (s, 1H, OH), 5.31 (s, 5H, C_5H_5), 5.68 (m, 1H, H-3), 7.46−7.77 (m, 10H, Ph). $^{13}C\{^1H\}$ NMR (75.4 MHz, acetone-d_6, 18 °C): δ 24.9 (s, $2CH_2$, −$(CH_2)_4$−), 27.3 (d, J_{CP} = 39.1 Hz, C-1), 38.9 (d, J_{CP} = 5.1 Hz, C-5), 39.2 (s, −$(CH_2)_4$−), 43.9 (d, J_{CP} = 28.0 Hz, C-2), 45.8 (s, −$(CH_2)_4$−), 83.4 (s, C-6), 83.8 (d, J_{CP} = 5.2 Hz, C-3), 85.9 (s, C_5H_5), 111.7 (s, C-4), 125.5−150.3 (Ph). $^{31}P\{^1H\}$ NMR (121.5 MHz, acetone-d_6, 18 °C): δ −59.2 (s). $C_{27}H_{30}F_6OP_2Ru$ (647.53 g/mol). MS (MALDI): *m*/*z* 503 [Ru(C_5H_5){Ph_2PCH_2CH═$CHC(C(C_4H_8)OH)$═CH_2}]$^+$. Yield of **6**: 48 mg, 70%. IR (KBr, $\nu(PF_6)$, cm^{-1}): 840. Molar conductivity (acetone, Ω^{-1} cm^2 mol^{-1}): 112. ^1H NMR (300.1 MHz, acetone-d_6, 18 °C): δ 0.75 (m, 1H, H-5 minor), 1.12 (m, 1H, H-5 major), 1.70 (s, 3H, CH_3 minor), 1.86 (s, 3H, CH_3 major), 2.90 (m, 3H, H-1 major + minor), 3.62 (d, J_{HH} = 4.7 Hz, 1H, H-5 minor), 3.95 (m, 1H, H-1 major+ minor), 4.04 (d, J_{HH} = 3.8 Hz, 1H, H-5 major), 4.72 (m, 1H, H-2 major), 4.84 (m, 1H, H-2 minor), 5.22 (s, 1H, OH major), 5.33 (s, 5H, C_5H_5 minor), 5.41 (s, 5H, C_5H_5 major), 5.47 (s, 1H, OH minor), 5.67 (m, 1H, H-3 major), 5.87 (m, 1H, H-3 minor), 7.27−7.79 (m, 30H, Ph). $^{13}C\{^1H\}$ NMR (75.4 MHz, acetone-d_6, 18 °C): δ 27.3 (d, J_{CP} = 39.5 Hz, C-1 minor), 27.4 (d, J_{CP} = 38.7 Hz, C-1 major), 39.1 (d, J_{CP} = 5.2 Hz, C-5 minor), 40.3 (d, J_{CP} = 5.1 Hz, C-5 major), 43.3 (d, J_{CP} = 28.3 Hz, C-2 minor), 43.8 (d, J_{CP} = 28.2 Hz, C-2 major), 75.7 (s, C-6 minor), 76.1 (s, C-6 major), 84.3 (d, J_{CP} = 5.2 Hz, C-3 minor), 85.4 (d, J_{CP} = 5.5 Hz, C-3 major), 86.4 (s, C_5H_5 minor), 86.5 (s, C_5H_5 major), 113.5 (s, C-4 minor), 113.8 (s, C-4 major), 125.3−149.4 (Ph). $^{31}P\{^1H\}$ NMR (121.5 MHz, acetone-d_6, 18 °C): δ −59.7 (s, minor), −60.2 (s, major). $C_{30}H_{30}F_6OP_2Ru$ (683.57 g/mol). MS (MALDI): *m*/*z* 539 [Ru(C_5H_5){Ph_2PCH_2CH═$CHC(RCMePh)$═CH_2}]$^+$.

Synthesis of [Ru(η^5-C_5H_5){κ(*P*)-η^4-(3Z)-$Ph_2PCH_2CH_2CH$═$CHC(R)$═CH_2}][PF_6] (R = CPh_2OH (7), $C(C_4H_8)OH$ (8), CMePhOH (9a,b), CHPhOH (10a,b)). A solution of [Ru(η^5-C_5H_5){κ^3(*P*,*C*,*C*)-$Ph_2PCH_2CH_2CH$═CH_2}(MeCN)][PF_6] (59 mg, 0.1 mmol) and the corresponding propargyl alcohol (0.4 mmol) in THF (10 mL) was refluxed for 1.5 h. The solution was then evaporated to dryness, the crude product extracted with dichloromethane (2 × 10 mL), and the extract filtered. Concentration of the resulting solution to ca. 3 mL followed by the addition of 30 mL of diethyl ether afford complexes **7**−**10** as white solids, which were washed with diethyl ether (2 × 5 mL) and vacuum-dried. The complexes **9a**,**b** and **10a**,**b** were separated by recrystallization from CH_2Cl_2/Et_2O, yielding white crystals of **9a** and **10b**, respectively. The corresponding solutions contained the complexes **9b** and **10a**, which were isolated by precipitation with *n*-hexane. Yield of **7**: 61 mg, 80%. IR (KBr, $\nu(PF_6)$, cm^{-1}): 841. Molar conductivity (acetone, Ω^{-1} cm^2 mol^{-1}): 126. ^1H NMR (400.1 MHz, acetone-d_6, 18 °C): δ 1.35 (dd, J_{HP} = 18.1 Hz, J_{HH} = 4.8 Hz, 1H, H-6), 1.41 (m, 1H, H-2), 2.52 (m, 1H, H-2), 3.00 (d, J_{HH} = 4.8 Hz, 1H, H-6), 3.60 (m, 1H, H-1), 3.76 (m, 1H, H-1), 5.12 (s, 5H, C_5H_5), 5.51 (m, 1H, H-3), 6.06 (d, J_{HH} = 8.1 Hz, 1H, H-4), 6.09 (s, 1H, OH), 7.22−7.78 (m, 20H, Ph). $^{13}C\{^1H\}$ NMR (100.6 MHz, acetone-d_6, 18 °C): δ 26.4 (d, J_{CP} = 7.0 Hz, C-2), 44.4 (d, J_{CP} = 6.0 Hz, C-6), 47.1 (d, J_{CP} = 35.2 Hz, C-1), 77.7 (s, C-3), 82.2 (s, C-7), 84.4 (s, C-4), 88.5 (s, C_5H_5), 117.1 (s, C-5), 127.7−149.0 (Ph). $^{31}P\{^1H\}$ NMR (162.0 MHz, acetone-d_6, 18 °C): δ 94.7 (s). Anal. Calcd for $C_{36}H_{34}F_6OP_2Ru$ (759.66 g/mol): C 56.92, H 4.51. Found: C 57.46, H 4.99. Yield of **8**: 55 mg, 83%. IR (KBr, $\nu(PF_6)$, cm^{-1}): 840. Molar conductivity (acetone, Ω^{-1} cm^2 mol^{-1}): 135. ^1H NMR (400.1 MHz, acetone-d_6, 18 °C): δ 0.88 (dd, J_{HP} = 16.8 Hz, J_{HH} = 4.5 Hz, 1H, H-6), 1.07 (m, 1H, H-2), 1.75 (m, 2H, −$(CH_2)_4$−), 2.07 (m, 6H, −$(CH_2)_4$−), 2.34 (m, 1H, H-2), 3.00 (d, J_{HH} = 4.5 Hz, 1H, H-6), 3.48 (m, 1H, H-1), 3.69 (m, 1H, H-1), 4.80 (s, 1H, OH), 5.17 (s, 5H, C_5H_5), 5.48 (m, 1H, H-3), 6.21 (d, J_{HH} = 8.2 Hz, 1H, H-4), 7.48−7.99 (m, 10H, Ph). $^{13}C\{^1H\}$ NMR (100.6 MHz, acetone-d_6, 18 °C): δ 24.9 (s, −$(CH_2)_4$−), 26.2 (d, J_{CP} = 7.5 Hz, C-2), 26.7 (s, −$(CH_2)_4$−), 40.1 (s, −$(CH_2)_4$−), 44.0 (s, C-6), 47.2 (d, J_{CP} = 34.3 Hz, C-1), 48.8 (s, −$(CH_2)_4$−), 78.9 (d, J_{CP} = 3.3 Hz, C-3), 81.9 (s, C-4), 84.8 (s, C-7), 88.3 (s, C_5H_5), 115.8 (s, C-5), 130.7−142.8 (Ph). $^{31}P\{^1H\}$ NMR (162.0 MHz, acetone-d_6, 18 °C): δ 93.5 (s). Anal. Calcd for $C_{28}H_{32}F_6OP_2Ru$ (661.56 g/mol): C 50.83, H 4.88. Found: C 51.41, H 5.31. Yield of **9a**: 24 mg, 34%. IR (KBr, $\nu(PF_6)$, cm^{-1}): 840. Molar conductivity (acetone, Ω^{-1} cm^2 mol^{-1}): 134. ^1H NMR (300.1 MHz, acetone-d_6, 18 °C): δ 0.80 (dd, J_{HP} = 18.0 Hz, J_{HH} = 4.3 Hz, 1H, H-6), 0.98 (m, 1H, H-2), 2.08 (s, 3H, CH_3), 2.40 (m, 1H, H-2), 2.94 (d, J_{HH} = 4.3 Hz, 1H, H-6), 3.46 (m, 1H, H-1), 3.66 (m, 1H, H-1), 5.17 (s, 5H, C_5H_5), 5.35 (s, 1H, OH), 5.55 (m, 1H, H-3), 6.34 (d, J_{HH} = 8.0 Hz, 1H, H-4), 7.26−7.83 (m, 15H, Ph). $^{13}C\{^1H\}$ NMR (75.4 MHz, acetone-d_6, 18 °C): δ 26.3 (d, J_{CP} = 7.5 Hz, C-2), 32.3 (s, CH_3), 40.8 (d, J_{CP} = 6.0 Hz, C-6), 47.0 (d, J_{CP} = 34.5 Hz, C-1), 77.2 (s, C-7), 78.2 (d, J_{CP} = 3.7 Hz, C-3), 83.5 (s, C-4), 88.5 (s, C_5H_5), 117.1 (s, C-5), 126.7−148.9 (Ph). $^{31}P\{^1H\}$ NMR (162.0 MHz, acetone-d_6, 18 °C): δ 95.1 (s). Anal. Calcd for $C_{31}H_{32}F_6OP_2Ru{\cdot}CH_2Cl_2$ (782.52 g/mol): C 49.12, H 4.38. Found: C 49.36, H 4.28. Yield of **9b**: 16 mg, 24%. IR (KBr, $\nu(PF_6)$, cm^{-1}): 839. Molar conductivity (acetone, Ω^{-1} cm^2 mol^{-1}): 122. ^1H NMR (300.1 MHz, acetone-d_6, 18 °C): δ 0.85 (m, 1H, H-2), 1.02 (dd, J_{HP} = 17.4 Hz, J_{HH} = 4.9 Hz, 1H, H-6), 1.83 (s, 3H, CH_3), 2.25 (m, 1H, H-2), 3.36 (d, J_{HH} = 4.9 Hz, 1H, H-6), 3.48 (m, 1H, H-1), 3.67 (m, 1H, H-1), 5.29 (s, 5H, C_5H_5), 5.44 (m, 2H, H-3, OH), 6.24 (d, J_{HH} = 8.3 Hz, 1H, H-4), 7.23−8.02 (m, 15H, Ph). $^{13}C\{^1H\}$ NMR (75.4 MHz, acetone-d_6, 18 °C): δ 26.2 (d, J_{CP} = 7.6 Hz, C-2), 28.7 (s, CH_3), 40.9 (d, J_{CP} = 5.8 Hz, C-6), 47.1 (d, J_{CP} = 34.4 Hz, C-1), 77.5 (s, C-7), 78.5 (d, J_{CP} = 4.0 Hz, C-3), 81.7 (s, C-4), 88.6 (s, C_5H_5), 117.2 (s, C-5), 127.1−150.7 (Ph). $^{31}P\{^1H\}$ NMR (162.0 MHz, acetone-d_6, 18 °C): δ 94.2 (s). Anal. Calcd for $C_{31}H_{32}F_6OP_2Ru$ (697.59 g/mol): C 53.37, H 4.62. Found: C 54.12, H 4.91. Yield of **10a**: 32 mg, 47%. IR (KBr, $\nu(PF_6)$, cm^{-1}): 838. Molar conductivity (acetone, Ω^{-1} cm^2 mol^{-1}): 110. ^1H NMR (300.1 MHz, acetone-d_6, 18 °C): δ 0.74 (m, 1H, H-2), 0.87 (m, 1H, H-6), 2.30 (m, 1H, H-2), 3.20 (d, J_{HH} = 4.0 Hz, 1H, H-6), 3.51 (m, 2H, H-1), 5.24 (s, 6H, OH, C_5H_5), 5.48 (m, 1H, H-3), 5.62 (br, 1H, H-7), 6.49 (d, J_{HH} = 8.1 Hz, 1H, H-4), 7.28−8.00 (m, 15H, Ph). $^{13}C\{^1H\}$ NMR (100.6 MHz, acetone-d_6, 18 °C): δ 26.8 (d, J_{CP} = 8.4 Hz, C-2), 42.5 (d, J_{CP} = 5.2 Hz, C-6), 47.2 (d, J_{CP} = 33.4 Hz, C-1), 78.4, 79.4, 82.3 (3 x s, C-3,4,7), 89.2 (s, C_5H_5), 110.7 (s, C-5), 128.5−147.5 (Ph). $^{31}P\{^1H\}$ NMR (162.0 MHz, acetone-d_6, 18 °C): δ 92.5 (s). Anal. Calcd for

$C_{30}H_{30}F_6OP_2Ru$ (683.57 g/mol): C 52.71, H 4.42. Found: C 53.25, H 4.98. Yield of **10b**: 24 mg, 35%. IR (KBr, ν (PF_6), cm^{-1}): 840. Molar conductivity (acetone, Ω^{-1} cm^2 mol^{-1}): 117. ^1H NMR (300.1 MHz, acetone-d_6, 18 °C): δ 0.75 (m, 1H, H-2), 0.98 (dd, J_{HP} = 16.2 Hz, J_{HH} = 3.5 Hz, 1H, H-6), 2.25 (m, 1H, H-2), 3.50 (m, 2H, H-1), 3.64 (m, 1H, H-6), 5.17 (s, 5H, C_5H_5), 5.23 (s, 1H, OH), 5.51 (m, 1H, H-3), 5.70 (br, 1H, H-7), 6.16 (d, J_{HH} = 7.9 Hz, 1H, H-4), 7.30−8.03 (m, 15H, Ph). $^{13}C\{^1H\}$ NMR (100.6 MHz, acetone-d_6, 18 °C): δ 26.6 (d, J_{CP} = 8.0 Hz, C-2), 39.1 (d, J_{CP} = 5.3 Hz, C-6), 47.3 (d, J_{CP} = 33.6 Hz, C-1), 78.1 (s, C-4,7), 80.2 (d, J_{CP} = 3.8 Hz, C-3), 86.5 (s, C-4,7), 89.2 (s, C_5H_5), 111.5 (s, C-5), 128.6−146.8 (Ph). $^{31}P\{^1H\}$ NMR (162.0 MHz, acetone-d_6, 18 °C): δ 92.4 (s). Anal. Calcd for $C_{30}H_{30}F_6OP_2Ru$ (683.57 g/mol): C 52.71, H 4.42. Found: C 52.73, H 4.79.

Synthesis of [Ru(η^5-C_5H_5){κ(*P*)-η^4-(2*Z*,4*E*)-Ph_2PCH_2CH=$CHCH$=$CH(R)$}][PF_6] (R = Ph (11), R = *p*-MeC_6H_4 (12)). A solution of [Ru(η^5-C_5H_5){κ^3(*P*,*C*,*C*)-Ph_2PCH_2CH=CH_2}(MeCN)]-[PF_6] (58 mg, 0.1 mmol) and the corresponding alkyne (0.3 mmol) in THF (10 mL) was refluxed for 50 min. The solution was then evaporated to dryness, the crude product extracted with dichloromethane (2 × 10 mL), and the extract filtered. Concentration of the resulting solution to ca. 3 mL followed by the addition of 30 mL of diethyl ether afforded complexes **11** and **12** as pale yellow solids, which were washed with diethyl ether (2 × 5 mL) and vacuum-dried. Yield of **11**: 45 mg, 77%. IR (KBr, ν(PF_6), cm^{-1}): 838. Molar conductivity (acetone, Ω^{-1} cm^2 mol^{-1}): 101. ^1H NMR (300.1 MHz, acetone-d_6, 18 °C): δ 2.90 (dd, J_{HP} = 15.5 Hz, J_{HH} = 9.5 Hz, 1H, H-5), 3.29 (m, 1H, H-1), 4.01 (m, 1H, H-1), 4.98 (m, 1H, H-2), 5.24 (s, 5H, C_5H_5), 5.71 (m, 1H, H-3), 6.60 (d, J_{HH} = 7.3 Hz, 1H, Ph), 6.97 (dd, J_{HH} = 9.5 Hz, J_{HH} = 6.5 Hz, 1H, H-4), 6.94−7.84 (m, 15 H, Ph). $^{13}C\{^1H\}$ NMR (100.6 MHz, acetone-d_6, 18 °C): δ 28.1 (d, J_{CP} = 37.9 Hz, C-1), 49.8 (d, J_{CP} = 26.8 Hz, C-2), 66.5, 83.3 (2 × s, C-4,5), 86.4 (d, J_{CP} = 6.5 Hz, C-3), 87.9 (s, C_5H_5), 127.4−141.6 (Ph). $^{31}P\{^1H\}$ NMR (121.5 MHz, acetone-d_6, 18 °C): δ −64.6 (s). $C_{28}H_{26}F_6P_2Ru$ (639.51 g/mol). MS (FAB+): *m*/*z* 495 [Ru(C_5H_5){Ph_2PCH_2CH=$CHCH$=CH-(Ph)}]$^+$. Yield of **12**: 44 mg, 69%. IR (KBr, ν(PF_6), cm^{-1}): 839. Molar conductivity (acetone, Ω^{-1} cm^2 mol^{-1}): 98. ^1H NMR (300.1 MHz, acetone-d_6, 18 °C): δ 2.23 (s, 3H, CH_3), 2.91 (dd, J_{HP} = 15.4 Hz, J_{HH} = 9.7 Hz, 1H, H-5), 3.26 (m, 1H, H-1), 3.99 (m, 1H, H-1), 4.95 (m, 1H, H-2), 5.23 (s, 5H, C_5H_5), 5.70 (m, 1H, H-3), 6.49 (d, J_{HH} = 8.2 Hz, 1H, Ph), 6.91 (m, 2H, H-4, Ph), 6.97−7.83 (m, 14H, Ph). $^{13}C\{^1H\}$ NMR (75.4 MHz, acetone-d_6, 18 °C): δ 22.1 (s, CH_3), 28.7 (d, J_{CP} = 37.9 Hz, C-1), 50.2 (d, J_{CP} = 27.4 Hz, C-2), 68.9, 86.6 (2 × s, C-4,5), 86.9 (d, J_{CP} = 7.0 Hz, C-3), 88.4 (s, C_5H_5), 127.6−139.2 (Ph). $^{31}P\{^1H\}$ NMR (121.5 MHz, acetone-d_6, 18 °C): δ −64.3 (s). $C_{29}H_{28}F_6P_2Ru$ (653.54 g/mol). MS (FAB+): *m*/*z* 509 [Ru(C_5H_5){Ph_2PCH_2CH=$CHCH$=CH-(MeC_6H_4)}]$^+$.

Theoretical Calculations. All the minimum-energy structures reported herein were optimized using hybrid density functional theory (DFT), within the Gaussian03 program,[11] using Becke's three-parameter hybrid exchange−correlation functional[12] containing the B3LYP nonlocal gradient correction.[13] The LANL2DZ basis set, with relativistic effective core potentials, was used for the Ru atoms.[14] The basis set used for the remaining atoms was the 6-31G, with addition of (d,p)-polarization for all atoms. All optimized structures were confirmed as minima by calculation of analytical frequencies. For each calculation, the input model molecule was based on one of the X-ray-determined structures reported in this article, conveniently modified (if necessary) by changing the appropriate R groups.

X-ray Crystal Structure Determination of Complexes 9a·1/2OEt_2, 9b, 10b·1/2OEt_2, and 12. Crystals suitable for X-ray diffraction analysis were obtained by slow diffusion of diethyl ether (**9a**, **9b**, and **10b**) or *n*-hexane (**12**) into a saturated solution of the corresponding complex in dichloromethane.

The most relevant crystal and refinement data are collected in Table 3. Data collection were performed on a Bruker SMART 6K CCD area-detector three-circle diffractometer (Cu Kα radiation, λ = 1.5418 Å).[15] X-ray data were collected at 100(2) K, with a combination of three runs at different φ and 2θ angles. The data were collected using 0.3° wide ω scans with a crystal-to-detector distance of 40 mm. The diffraction frames were integrated using the SAINT package[16] and corrected for absorption with SADABS.[17] For **12** data were collected at 150(2) K on a Nonius Kappa CCD single-crystal diffractometer using Cu Kα radiation (λ = 1.5418 Å) with a crystal−detector distance fixed at 29 mm, using the oscillation method, with 2° oscillation. Data colletion strategy was calculated with the program COLLECT.[18] Data reduction and cell refinement were performed with the programs HKL Denzo and Scalepack,[19] and absorption correction was applied by means of SORTAV.[20]

The software package WINGX was used for space group determination and structure solution and refinement.[21] The structures were solved by Patterson interpretation and phase expansion using DIRDIF.[22] Isotropic least-squares refinement on F^2 was performed using SHELXL97.[23] For **9a** and **10b**, one diethyl ether molecule of solvation for two formula units of the complex was found to be disordered over two positions with 0.5 site occupancy factors. During the final stages of the refinements, all the positional parameters and the anisotropic temperature factors of all the non-H atoms were refined with the exception of those from the disordered diethyl ether solvent molecule in **10b**, which were isotropically refined. The H atoms were geometrically located and their coordinates were refined riding on their parent atoms, except for the H atoms of the molecules **10b** and **12** and for H1A and H1B of **9a**, where the coordinates of H atoms were found from difference Fourier maps and included in a refinement with isotropic parameters. In all cases, the maximum residual electron density is located near heavier atoms, except for **10b**, in which the highest residual peaks are close to the disordered solvent molecule. The function minimized was $([\sum wF_o^2 - F_c^2)/\sum w(F_o^2)]^{1/2}$, where $w = 1/[\sigma^2(F_o^2)$

(11) Frisch, M. J.; Trucks, G. W.; Schlegel, H. B.; Scuseria, G. E.; Robb, M. A.; Cheeseman, J. R.; Montgomery, J. A.; Vreven, T.; Kudin, K. N.; Burant, J. C.; Millam, J. M.; Iyengar, S. S.; Tomasi, J.; Barone, V.; Mennucci, B.; Cossi, M.; Scalmani, G.; Rega, N.; Petersson, G. A.; Nakatsuji, H.; Hada, M.; Ehara, M.; Toyota, K.; Fukuda, R.; Hasegawa, J.; Ishida, M.; Nakajima, T.; Honda, Y.; Kitao, O.; Nakai, H.; Klene, M.; Li, X.; Knox, J. E.; Hratchian, H. P.; Cross, J. B.; Adamo, C.; Jaramillo, J.; Gomperts, R.; Stratmann, R. E.; Yazyev, O.; Austin, A. J.; Cammi, R.; Pomelli, C.; Ochterski, J. W.; Ayala, P. Y.; Morokuma, K.; Voth, G. A.; Salvador, P.; Dannenberg, J. J.; Zakrzewski, V. G.; Dapprich, S.; Daniels, A. D.; Strain, M. C.; Farkas, O.; Malick, D. K.; Rabuck, A. D.; Raghavachari, K.; Foresman, J. B.; Ortiz, J. V.; Cui, Q.; Baboul, A. G.; Clifford, S.; Cioslowski, J.; Stefanov, B. B.; Liu, G.; Liashenko, A.; Piskorz, P.; Komaromi, I.; Martin, R. L.; Fox, D. J.; Keith, T.; Al-Laham, M. A.; Peng, C. Y.; Nanayakkara, A.; Challacombe, M.; Gill, P. M. W.; Johnson, B.; Chen, W.; Wong, M. W.; Gonzalez, C.; Pople, J. A. *Gaussian03*; Gaussian, Inc.: Wallingford, CT, 2004.

(12) Becke, A. D. *J. Chem. Phys.* **1993**, *98*, 5648−5652.

(13) Lee, C.; Yang, W.; Parr, R. G. *Phys. Rev. B* **1988**, *37*, 785−789.

(14) Hay, P. J.; Wadt, W. R. *J. Chem. Phys.* **1985**, *82*, 299−310.

(15) *SMART* version 5.625, Area-Detector Software Package; Bruker AXS; Madison, WI, 1997−2001.

(16) *SAINT* version 6.02; Bruker Analytical X-ray Systems: Madison, WI, 2000.

(17) Sheldrick, G. M. *SADABS* empirical absorption program; University of Gottingen, 1996.

(18) *Collect*; Nonius BV: Delft, 1997−2000.

(19) Otwinowski, Z.; Minor, W. *Methods Enzymol*. **1997**, *276*, 307−326.

(20) Blessing, R. H. *Acta Crystallogr. Sect. A* **1995**, *51*, 33−38.

(21) Farrugia, L. J. *J. Appl. Crystallogr*. **1999**, *32*, 837−838.

(22) Beurskens, P. T.; Admiraal, G.; Beurskens, G.; Bosman, W. P.; García-Granda, S.; Gould, R. O.; Smits J. M. M.; Smykalla, C. *The DIRDIF Program System*; Techical Report of the Crystallographic Laboratory; University of Nijimegen: Nijimegen, The Netherlands, 1999.

(23) Sheldrick, G. M. *SHELXL-97*, Program for the Refinement of Crystal Structures; University of Göttingen, 1997.

Table 3. Crystal Data and Structure Refinement Details for Complexes 9a·1/2OEt$_2$, 9b, 10b·1/2OEt$_2$, and 12

	9a·1/2OEt$_2$	**9b**	**10b·1**/2OEt$_2$	**12**
chemical formula	2($C_{31}H_{32}OPRu$), 2(F_6P), $C_4H_{10}O$	$C_{31}H_{32}F_6OP_2Ru$	2($C_{30}H_{30}OPRu$), 2(F_6P), $C_4H_{10}O$	$C_{29}H_{28}F_6P_2Ru$
fw	1469.27	697.58	1441.22	653.52
T (K)	100(2)	100(2)	100(2)	150(2)
wavelength (Å)	1.5418	1.5418	1.5418	1.5418
cryst syst	monoclinic	monoclinic	monoclinic	monoclinic
space group	$P2_1/c$	Cc	$P2_1/n$	$P2_1/c$
a (Å)	13.1933(5)	10.6948(2)	16.1051(2)	9.41650(10)
b (Å)	11.7672(5)	38.0333(8)	11.7230(2)	18.1360(2)
c (Å)	21.0420(7)	15.2449(2)	17.6605(2)	16.3007(2)
β (deg)	105.379(2)	110.0030(10)	106.5630(10)	106.8660(10)
V (Å^3)	3149.8(2)	5826.92(18)	3195.95(8)	2664.05(5)
Z	2	8	2	4
ρ_{calcud} (g cm^{-3})	1.549	1.590	1.498	1.629
μ (mm^{-1})	5.449	5.953	5.457	6.437
F(000)	1500	2832	1468	1320
cryst size (mm)	0.09 × 0.05 × 0.02	0.08 × 0.06 × 0.04	0.15 × 0.09 × 0.06	0.5 × 0.45 × 0.45
θ range (deg)	3.47−69.49	2.32−71.22	3.28−71.23	5.48 to 70.12
index ranges	$-16 \le h \le 14$ $-14 \le k \le 13$ $-25 \le l \le 24$	$-13 \le h \le 12$ $-42 \le k \le 44$ $-18 \le l \le 16$	$-19 \le h \le 19$ $-14 \le k \le 14$ $-21 \le l \le 20$	$-11 \le h \le 10$ $0 \le k \le 22$ $0 \le l \le 19$
no. reflns collected	18 475	21 931	29 361	39 332
no. unique reflns	5683 [R(int) = 0.0724]	8681 [R(int) = 0.0658]	6099 [R(int) = 0.0456]	4945 [R(int) = 0.047]
completeness to θ_{max}	96.2%	96.9%	98.4%	97.7%
no. params/ restraints	425/0	741/0	501/3	455/0
goodness-of-fit on F^2	1.012	1.021	1.034	1.098
wt function (a, b)	0.0626, 1.1655	0.0594, 0	0.0904, 14.6994	0.0497, 4.8305
R_1 [I > 2ρ(I)]	R_1 = 0.0494	R_1 = 0.0504	R_1 = 0.0527	R_1 = 0.0356
wR_2 [I > 2ρ(I)]	wR_2 = 0.1103	wR_2 = 0.1150	wR_2 = 0.1461	wR_2 = 0.0930
R_1(all data)	R_1 = 0.0782	R_1 = 0.0600	R_1 = 0.0590	R_1 = 0.0364
wR_2(all data)	wR_2 = 0.1230	wR_2 = 0.1204	wR_2 = 0.1526	wR_2 = 0.0935
largest diff peak and hole (e Å^3)	0.826 and −0.518	1.112 and −0.354	3.877 and −0.668	0.894 and −0.841

+ (aP)^2 + bP] (a and b values are collected in Table 3) with $\sigma(F_o^2)$ from counting statistics and P = (Max(F_o^2, 0) + 2F_c^2)/3. Atomic scattering factors were taken from the International Tables for X-ray Crystallography.[24] Geometrical calculations were made with PARST.[25] The crystallographic plots were made with PLATON.[26]

CCDC-646912 (**9a**), CCDC-646913 (**9b**), CCDC-646914 (**10b**), and CCDC-646915 (**12**) contain the supplementary crystallographic data for this paper. These data can be obtained free of charge from The Cambridge Crystallographic Data Centre via www.ccdc.cam.ac.uk/data_request/cif.

Acknowledgment. This work was supported by the Spanish MCT (research project BQU2003-00255 and MAT2006-01997 (E.P.-C.) and Principado de Asturias (PR-01-GE-6). A.V. thanks the Spanish Ministerio de Educación, Cultura y Deporte for a scholarship.

Supporting Information Available: Computer-generated plots and atomic coordinates for all the DFT-optimized molecular structures and ^{1}H, ^{31}P{^{1}H}, and ^{13}C{^{1}H} NMR spectra are available free of charge via the Internet at http://pubs.acs.org.

OM700476F

(24) *International Tables for X-Ray Crystallography*; Kynoch Press: Birmingham, 1974; Vol. IV (Present distrubutor: Kluwer Academic Publishers, Dordrecht).

(25) Nardelli, M. *Comput. Chem.* **1983**, *7*, 95−98.

(26) Spek, A. L. *PLATON*, a multipurpose crystallographic tool; Utrecht University: Utrecht, The Netherlands, 2006.